BIOCHEMISTRY
including biophysical chemistry & molecular biology

Article

pubs.acs.org/biochemistry

Mapping a Ketosynthase:Acyl Carrier Protein Binding Interface via Unnatural Amino Acid-Mediated Photo-Cross-Linking

Zhixia Ye† and Gavin J. Williams*

Department of Chemistry, North Carolina State University, Raleigh, North Carolina 27695, United States

Supporting Information

ABSTRACT: Probing and interrogating protein interactions that involve acyl carrier proteins (ACP's) in fatty acid synthases and polyketide synthases are critical to understanding the molecular basis for the programmed assembly of complex natural products. Here, we have used unnatural amino acid mutagenesis to site specifically install photo-cross-linking functionality into acyl carrier proteins from diverse systems and the ketosynthase FabF from the *Escherichia coli* type II fatty acid synthase. Subsequently, a photo-cross-linking assay was employed to systematically probe the ability of FabF to interact with a broad panel of ACP's, illustrating the expected orthogonality of ACP:FabF interactions and the role of charged residues in helix II of the ACP. In addition, FabF residues involved in the binding interaction with the cognate carrier protein were identified via surface scanning mutagenesis and photo-cross-linking. Furthermore, the ability to install the photo-cross-linking amino acid at virtually any position allowed interrogation of the role that carrier protein acylation plays in determining the binding interface with FabF. A conserved carrier protein motif that includes the phosphopantetheinylation site was also shown to play an integral role in maintenance of the AcpP:FabF binding interaction. Our results provide unprecedented insight into the molecular details that describe the AcpP:FabF binding interface and demonstrate that unnatural amino acid based photo-cross-linking is a powerful tool for probing and interrogating protein interactions in complex biosynthetic systems.

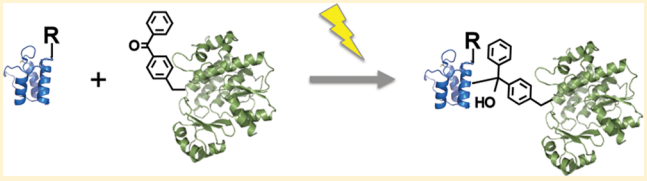

Fatty acids and polyketides are types of natural products biosynthesized by fatty acid synthases (FAS's) and polyketide synthases (PKS's), respectively. FAS's and PKS's are classified into various groups according to the organization and structural arrangement of the enzymatic components.[1] Type I systems are large multidomain protein assemblies. In type I FAS's, all of the domains are located on a single polypeptide, whereas for type I PKS's, modules of domains are responsible for selection, installation, and tailoring of each ketide. Fungal PKS's also belong to the type I family but are nonmodular and act iteratively. In contrast, type II systems consist of enzyme activities that are located on separate polypeptides. Type II FAS's involve the iterative action of each enzyme to construct the final fatty acid in which every acyl building block is fully reduced. In type II PKS's, building block acyl groups are not always full reduced. Finally, type III PKS's, which include the "chalcone synthase" family, use acyl-coenzyme A (CoA) substrates directly, without the use of an acyl carrier protein (ACP)[2] (although exceptions are known[3]), via a single active site.

Delicately orchestrated interactions between the ACP and other interacting domains are critical to the catalytic cycle of both type I and type II FAS's/PKS's. For example, in type II FAS's and PKS's, the ACP is required to interact *in trans* with every other domain. Notably, chain elongation is facilitated by interactions between ACP and ketosynthase (KS) domains of the FAS (Figure 1A). Determining the molecular recognition details that govern such processes is critical to understanding the catalytic processes that occur during PKS and FAS biosynthesis.[4,5] Interaction between these domains is likely programmed via recognition of the acyl substrates and/or specific binding interfaces between the ACP/KS. However, the requisite weak and transient nature of such interactions[6] renders crystallographic analysis a difficult method to provide such information. Consequently, mechanism-based cross-linkers have been used to interrogate various ACP interactions, including those with KS's, and to obtain stunning structural snapshots of the interaction between the *Escherichia coli* (*E. coli*) FAS carrier protein (AcpP) and dehydratase, FabA.[4] Mutagenic studies have implicated helix II of ACP as being an important recognition motif for the ACP:KS interaction,[7] as well as interactions between other domains,[8,9] and ACP:FabH docking simulations have provided further evidence of the general involvement of this motif.[6] To date though, there are no reported crystal structures of complexes between an ACP and KS of any type II PKS or FAS. Moreover, almost nothing is known regarding the precise ACP:KS binding interface[5] or how the carrier protein acyl group impacts recognition by the KS.

Previously, we have reported the use of unnatural amino acid mutagenesis to install the photo-cross-linking amino acid *p*-benzoyl-L-phenylalanine (pBpa) in place of the phosphopantetheine prosthetic arm of several ACP's.[10] This enabled detection and quantification of ACP:KS interactions by SDS-

Received: July 29, 2014
Revised: November 7, 2014
Published: November 26, 2014

   dx.doi.org/10.1021/bi500936u | *Biochemistry* 2014, 53, 7494−7502

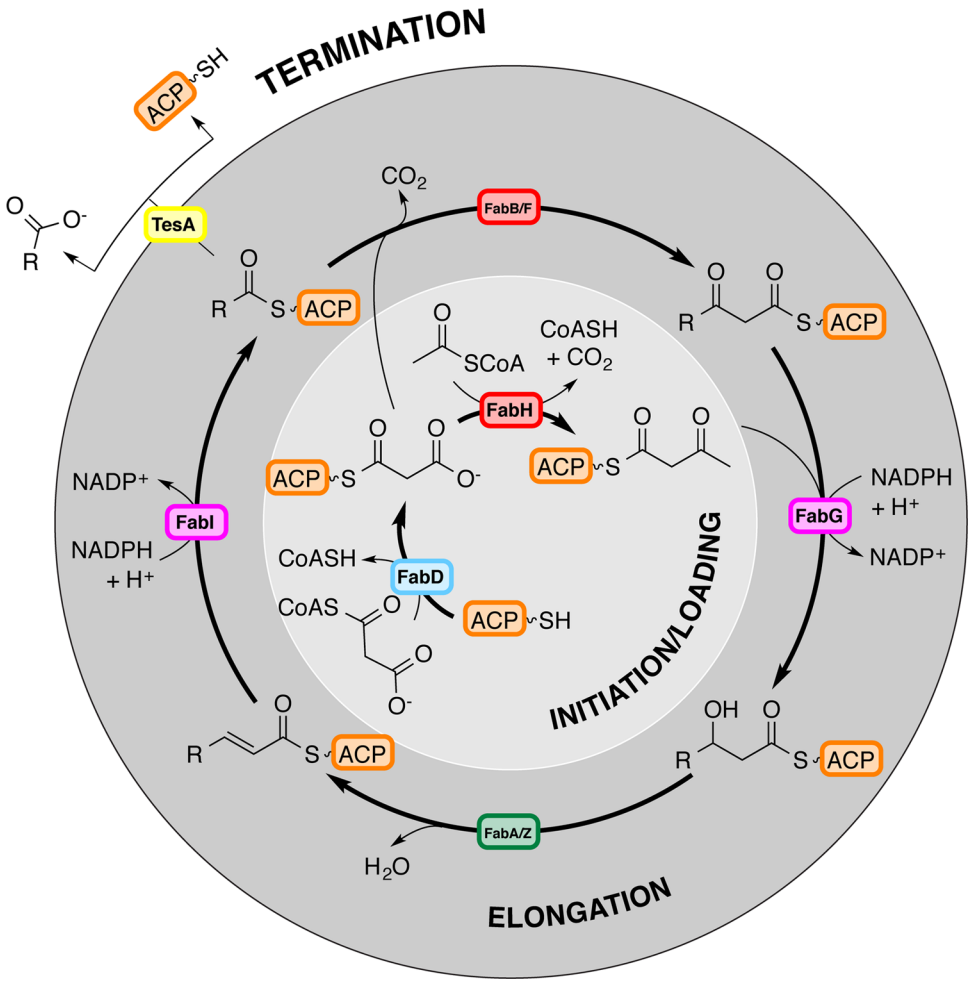

Figure 1. Biosynthesis of saturated fatty acids in *E. coli*. The ketosynthases involved with chain elongation are highlighted in red.

PAGE analysis of photo-cross-linked products (Figure 2). Here, this approach was expanded and modified in order to interrogate with high precision the interaction between the *E. coli* FAS AcpP and the corresponding cognate KS, FabF (β-ketoacyl-ACP synthase, KAS II). This approach was used to (i) demonstrate orthogonality of ACP:FabF interactions using a comprehensive panel of carrier proteins, (ii) map the AcpP:FabF binding interface with single residue resolution, and (iii) probe the contribution of a carrier protein conserved motif and acyl identity to AcpP:FabF interactions. Cumulatively, these data provided unprecedented insight into the interaction between a FAS carrier protein and KS, and established unnatural amino acid mediated photo-cross-linking as a versatile platform for probing protein interactions in complex biosynthetic apparatus.

MATERIALS AND METHODS

Materials. Reagents were of the highest-grade possible and purchased from Sigma, unless otherwise indicated. Isopropyl β-D-thiogalactoside (IPTG) was from Calbiochem. Primers were ordered from Integrated DNA Technologies. pBpa was from PepTech Corp. Bacterial strain *E. coli* BL21(DE3) competent cells was from Promega.

Plasmid Construction. pEVOL-pBpa plasmid was kindly provided by the Schultz laboratory at the Scripps Research Institute (La Jolla, CA). Plasmids containing AcpP, $ACP2_{DEBS}$ and FabF were as previously described.[10] Genes encoding act-ACP and Sc-FAS-ACP were amplified by polymerase chain reaction from genomic DNA of *Streptomyces coelicolor* using primers listed in Table S1 of the Supporting Information. The PCR reaction mixture contained each primer at 2 μM, 0.25 mM each dNTP, 20 ng of genomic DNA, and 1 unit Phire Hot Start II DNA polymerase (Thermo Scientific), in buffer supplied by the manufacturer. Amplification involved an initial denaturation step at 98 °C for 3 min followed by cycling at 98 °C for 1 min, 60 °C for 1 min, and 72 °C for 1 min/kb for 30 cycles, and a final extension for 10 min at 72 °C. Purified PCR products were digested with 20 units each of *Nde*I and *Eco*RI (NEB) at 37 °C for 4 h, followed by agarose gel purification. Inserts were ligated into a purified pET28a fragment that had been digested with the same restriction enzymes. The resulting ligation product mixture was transformed into *E. coli* DH5α competent cells. Transformants were screened by restriction analysis and sequences confirmed by DNA sequencing (GENEWIZ) (Table S2). $ACP6_{DEBS}$ was amplified from genomic DNA of *Saccharopolyspora erythraea* (Table S1) and cloned into pET28a via *Nde*I and *Eco*RI sites as described above.

Site-Directed Mutagenesis. All site-directed mutagenesis was performed using the Quikchange II mutagenesis kit (Agilent Technologies), as described by the manufacturer. All mutants were confirmed by DNA sequencing.

Protein Expression and Purification. Ec-FAS-AcpP (AcpP) was expressed as previously described,[10] wild-type $ACP2_{DEBS}$, $ACP6_{DEBS}$, act-ACP, and Sc-FAS-ACP, were

dx.doi.org/10.1021/bi500936u | *Biochemistry* 2014, 53, 7494−7502

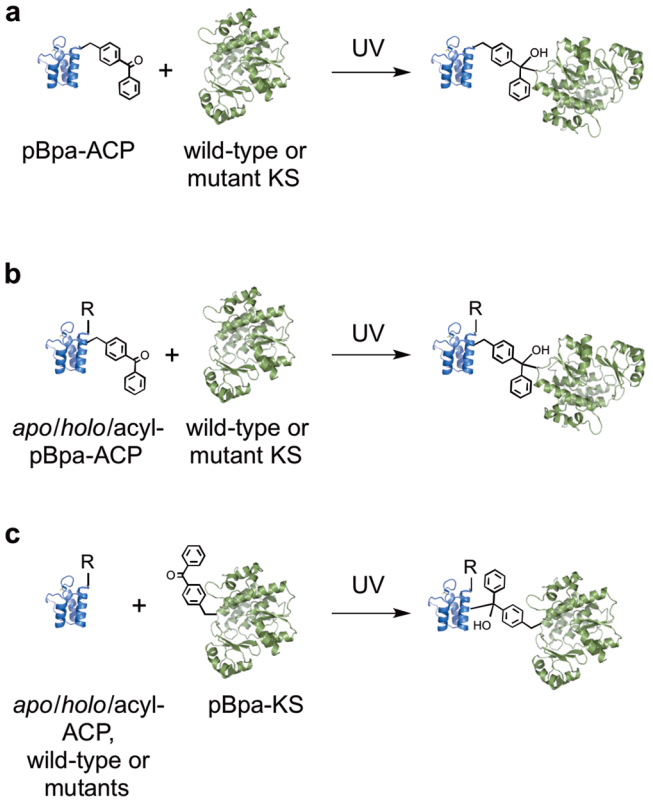

Figure 2. Probing ACP:KS protein interactions using unnatural amino acid mediated photo-cross-linking. (a) The ACP:KS interaction has been probed by installation of pBpa in place of the ACP phosphopantetheine prosthetic arm and assaying using KS surface mutants. (b) The impact of various ACP modifications on the ACP:KS interaction is probed by pBpa installation at a position other than the usual prosthetic arm site, followed by photo-cross-linking assay using KS surface mutants. (c) The ACP:KS interaction can be probed by pBpa installation in the KS domain and subsequent photo-cross-linking using various acylated forms of wild-type or surface mutant ACP's.

expressed using the same conditions as that for wild-type FabF.[10] pBpa-modified $ACP2_{DEBS}$, $ACP6_{DEBS}$, act-ACP, Sc-FAS-ACP, AcpP, and FabF (including all site-directed mutants) were expressed following the same procedure as AcpP-Ser36pBpa.[10] The phosphopantetheinyl transferase Sfp was overexpressed in *E. coli* BL21(DE3) as an N-terminally His_6-tagged fusion protein as previously described[11] and purified as reported earlier.[10]

Circular Dichroism Spectroscopy. Circular dichroism (CD) measurements were performed with a JASCO 810 CD Spectropolarimeter. Samples for CD were buffer exchanged into CD buffer (10 mM potassium phosphate, 50 mM sodium sulfate, pH 7.4),[12] and the concentration of samples was 0.2 mg/mL. Spectra from 190 to 260 nm were scanned at a step of 0.5 nm at 20 °C in a 0.1 cm cuvette, with 10 repeats. The scan speed was 100 nm/min.

Sfp-Catalyzed Formation of holo-ACP and acyl-ACP. Sfp-catalyzed holo- and acyl-ACP formation was performed in 100 μL of reaction mixture containing 50 mM Tris·HCl (pH 8.8), $MgCl_2$ (10 mM), DTT (5 mM), coenzyme A/acyl-coenzyme A (1 mM), apo-ACP (100 μM), and Sfp (20 μg) at 25 °C for 5 h. Production of holo- and acyl-ACP was confirmed by ESI-MS analysis of the crude product mixtures.

Photo-Cross-Linking. Photo-cross-linking reactions were carried out in a 96-well microtiter plate on ice. Reaction volume was 50 μL in PBS buffer and ACP's were provided in 5-fold excess of the KS (8.8 μM). Photo-cross-linking was initiated by irradiation at 365 nm with a hand-held UV lamp (6W, the plate was ∼3 cm away from the UV lamp) and then analyzed by SDS-PAGE (4−12% gradient). Photo-cross-linking efficiencies were expressed as a percentage conversion from the KS following densitometric analysis of the cross-linked product and monomeric KS, as previously described.[10]

RESULTS

Testing Putative Orthogonality of ACP:KS Interactions with a Panel of Diverse ACP's. Previously, only $ACP2_{DEBS}$ (ACP2 from the type I 6-deoxyerythronolide B synthase (DEBS) of *Saccharopolyspora erythraea*) and the type II FAS of *E. coli* (AcpP) were tested using our photo-cross-linking strategy.[10] Here, we expanded this panel of ACP's to include three additional carrier proteins: ACP6 from DEBS ($ACP6_{DEBS}$), the ACP from the type II actinorhodin PKS of *Streptomyces coelicolor* (act-ACP), and the ACP from the type II FAS of *S. coelicolor* (Sc-FAS-ACP). Site-directed mutagenesis was used to introduce the TAG amber suppression codon in place of the codon that encodes a conserved serine residue, which is the phosphopantetheinylation site (positions Ser45, Ser42, and Ser41, of $ACP6_{DEBS}$, act-ACP, and Sc-FAS-ACP, respectively, Table S2). Subsequently, following protein expression of each ACP mutant in the presence of pBpa, IPTG, and L-arabinose, the resulting ACP-pBpa mutants were purified by Ni-NTA chromatography, and the identity and purity of each mutant ACP were established by SDS-PAGE and ESI-MS analysis. The observed mass of each mutant ACP was in close agreement with that calculated from the corresponding theoretical amino acid sequence (Table S3), and ACP containing a natural amino acid at each TAG position could not be found by analysis of the ESI-MS spectra. The KS from the type II FAS (FabF) of *E. coli* was chosen as the potential interaction partner and was provided as a purified N-terminal hexa-histidine tagged fusion protein as previously described.[10]

Photo-cross-linking was then carried out using FabF and each pBpa-modified carrier protein by subjecting the reaction mixtures to UV irradiation at 365 nm. As previously reported, photo-cross-linked products were detected by SDS-PAGE analysis of the reaction mixtures and subsequently quantified by densitometric analysis of the cross-linked and monomeric species.[10] Photo-cross-linking efficiencies were expressed as a percentage of photo-cross-linked product, relative to the KS (which was the limiting reagent in each case). Photo-cross-linking was detected between FabF and $ACP6_{DEBS}$-Ser45pBpa (12%), Sc-FAS-ACP-Ser41pBpa (17%), and AcpP-Ser36pBpa (73%) (Table 1 and Figure S1). Sc-FAS-ACP has previously been suggested to interact with subunits of the *E. coli* FAS during fatty acid biosynthesis.[13] Photo-cross-linking was not observed for $ACP2_{DEBS}$-S50pBpa or act-ACP-S42pBpa (Table 1 and Figure S1). Helix II (H_{II}) of several ACP's has been suggested to be involved in the ACP:KS interaction,[6,14,15] and this region appears to be poorly conserved among the ACP's tested here (Figure S2). More specifically, H_{II} of AcpP and Sc-FAS-ACP contain several glutamate residues that are predicted to be involved in interactions with other domains (Figure S2). In contrast, $ACP6_{DEBS}$ presents an essentially neutral H_{II} surface, and the H_{II} surface of $ACP2_{DEBS}$ is positively charged (Figure S2). For act-ACP, the H_{II} surface is neutral overall, and

dx.doi.org/10.1021/bi500936u | *Biochemistry* 2014, 53, 7494−7502

Table 1. Cross-Linking Efficiency between FabF and Various ACP's[a]

carrier protein	cross-linking efficiency
$ACP2_{DEBS}$-S50pBpa	N.D.
Ec-FAS-AcpP-Ser36pBpa	73 ± 1.2
$ACP6_{DEBS}$-Ser45pBpa	12 ± 0.8
act-ACP-Ser42pBpa	N.D.
Sc-FAS-ACP-Ser41pBpa	17 ± 2.2
Ec-FAS-AcpP-Asn25pBpa	N.D.

[a]Each ACP was used in the apo form. Data are the average percent (%) photo-cross-linking activities of two independent measurements, error bars represent ±standard deviation from the mean (n = 2). N.D., not detected.

an arginine is present at the position equivalent to Glu49 in AcpP (Figure S2). The presence of positively charged or neutral residues in $ACP2_{DEBS}$ and act-ACP in place of key glutamic acid residues in H_{II} of AcpP might account for the failure to detect photo-cross-linking between FabF and $ACP2_{DEBS}$-S50pBpa or act-ACP-S42pBpa.

In order to provide further evidence that the photo-cross-linking assay faithfully reports ACP:KS interactions, pBpa was installed in AcpP at a position not expected to result in photo-cross-linking. Asn24 was chosen on the basis of the following observations. First, Asn24 is located on a face of AcpP distal to the conserved phosphopantetheinylation site, as judged by an AcpP crystal structure (Figure 3).[16] Second, while the pBpa

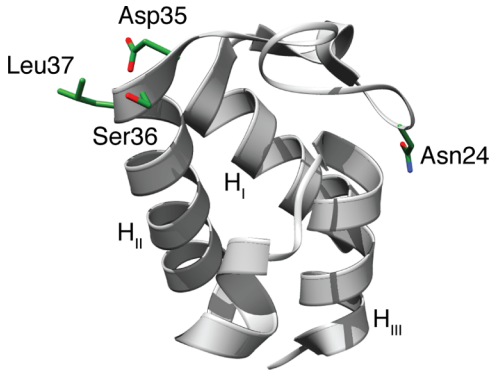

Figure 3. Crystal structure of AcpP (PDB ID 1T8K) highlighting the Asp-Ser-Leu motif and Asn24 as sticks. Each major helix is labeled.

reaction volume is estimated as a sphere with a 3.1 Å radius centered on the ketone oxygen,[17] the distance between the α-carbons of Asn24 and Ser36 is 18.5 Å (Figure 3). Third, although Asn24 is located in the middle of AcpP Loop I (L_I), molecular dynamics indicate Asn24 (and most of the loop) is remarkably static compared to the N-terminal and C-terminal regions of L_I in AcpP,[18] increasing the likelihood that Asn24 remains distal from the conserved Ser36. Accordingly, pBpa was incorporated in place of AcpP Asn24, and comparison of the AcpP-Asn24pBpa CD spectra to that of the wild-type AcpP indicated no significant structural changes upon introduction of the unnatural amino acid (Figure S3A). As expected, no photo-cross-linking was detected when AcpP-Asn24pBpa was subjected to UV irradiation in the presence of FabF (Table 1). This result emphasizes the accuracy with which specific ACP:KS interactions can be probed by carefully selecting the site of pBpa installation.

Mapping the FabF:AcpP Binding Interface. To map the epitope on FabF involved in the interaction with AcpP, and to dramatically expand upon our previous FabF mutagenesis,[10] a panel of 21 FabF mutants was first constructed, using a FabF crystal structure (Figure 4a) to select residues at the putative, vague AcpP binding area previously inferred.[19] This collection covered 13 unique surface residues and included introduction of amino acids with positive or negative charge (Lys, Glu) at selected residues in addition to substitution with alanine. The CD spectra for representative FabF mutants matched closely to that of the wild-type FabF spectra, suggesting conservation of secondary structures (Figure S3B). Subsequently, each FabF mutant was incubated with AcpP-Ser36pBpa and irradiated at 365 nm for 1 h.

The majority of the FabF mutants displayed >50% photo-cross-linking efficiency, as compared to the wild-type FabF (Figure 4b). Interestingly, two charged residues close to the putative AcpP interaction site, Glu225 and Asp227, displayed as much as 80% and 70% photo-cross-linking efficiency, respectively, when mutated to Ala, relative to wild-type FabF. To evaluate the potential influence of electrostatic properties at these two locations, Glu225 and Asp227 were replaced with amino acids with similar charge (Asp or Glu) or opposite charge (Lys). No significant changes in cross-linking efficiency were observed for these substitutions (Glu225Asp, Glu225Lys, Asp227Glu, and Asp227Lys) (Figure 4a,b), suggesting that Glu225 and Asp227 do not play a significant role in the FabF:AcpP binding interface. Significantly, two residues (Arg206 and Leu208) failed to yield a photo-cross-linked product upon mutagenesis to alanine. To further probe the importance of Arg206 and Leu208, each was mutated to Glu and Lys, respectively. Cross-linking could not be detected for the Arg206Glu, Arg206Lys, Leu208Glu, and Leu208Lys mutants, suggesting that positions 206 and 208 are highly sensitive to mutagenesis, with regard to recognition with AcpP. The FabF mutant Ser209Ala displayed 60% photo-cross-linking efficiency, as compared to the wild-type FabF, which is likely attributed to its close location to Arg206 and Leu208, which are likely the key interaction sites. Interestingly, substitution of Ala45 with Glu supported cross-linking at 50% the efficiency of the wild-type FabF, whereas substitution at the same position with Lys supports cross-linking at similar efficiency to that of the wild-type FabF. Thus, a neutral or positively charged residue is likely required at position 45 for efficient recognition with AcpP. As previously described, Ala substitution of the FabF residue Asn57, predicted to be distant from the putative AcpP binding site, failed to provide a significant impact on photo-cross-linking with AcpP, compared to wild-type FabF (Figure 4b). Taken together, the FabF surface mutagenesis data defines a specific set of residues that are required to form the FabF:AcpP binding interface (Figure 4a) and provides further evidence that Arg206 and Leu208 are key residues that contribute to recognition by AcpP.

Relocating the AcpP-pBpa Installation Site. It is not known whether FabF uses the same binding interface during the transacylation and condensation steps of the overall reaction catalyzed by this enzyme. In addition, the role that the AcpP-acyl moiety might play in determining the binding interface with FabF is unclear. These two aspects of FabF:AcpP recognition can be probed using unnatural amino acid based photo-cross-linking, since the phosphopantetheine prosthetic arm is available for acylation if pBpa is installed in proximity to AcpP Ser36. Accordingly, Asp35 and Leu37 of AcpP were

dx.doi.org/10.1021/bi500936u | Biochemistry 2014, 53, 7494−7502

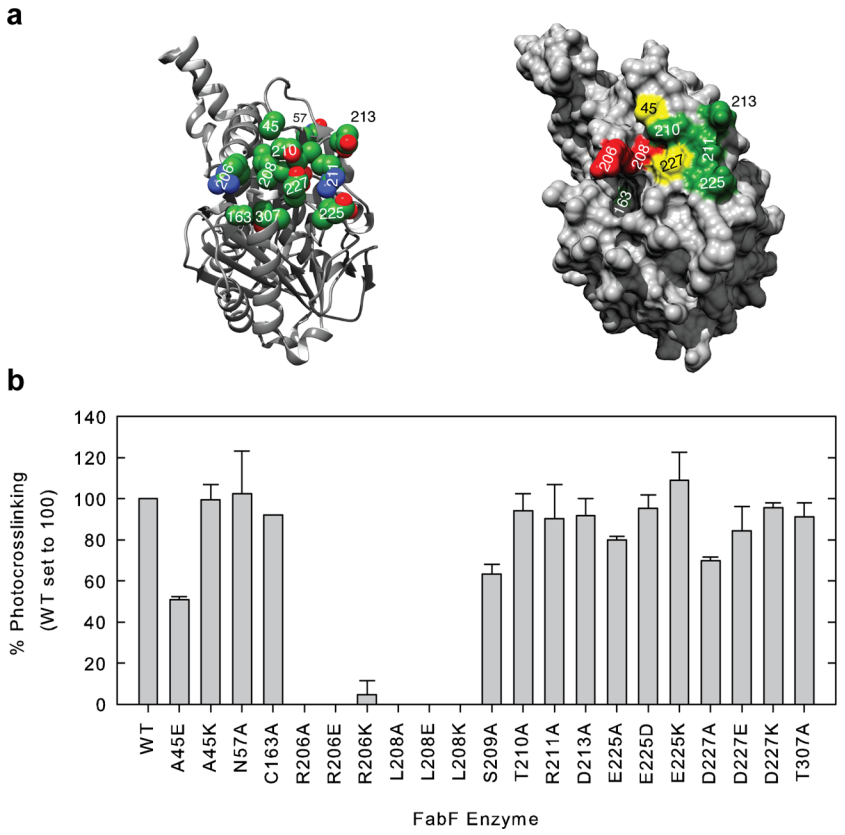

Figure 4. Mapping the FabF:AcpP binding interface by surface mutagenesis and photo-cross-linking. (a) Left, crystal structure of the Cys163Ala mutant of FabF (PDB ID 3I8P). Surface residues selected for mutagenesis are shown as spheres. Labels indicate residue number. Not every selected residue is visible. Right, photo-cross-linking activity of each corresponding alanine substitution mutant (except Ala45, which is A45E) using AcpP-Ser36pBpa, mapped onto a surface representation of FabF. Colors indicate photo-cross-linking activity relative to wild-type FabF: Red, <20% activity; yellow, 20−80% activity; green, >80% activity; gray, not determined. (b) Percentage (%) photo-cross-linking of wild-type or mutant FabF using AcpP-Ser36pBpa. Each bar is the average of two independent measurements. Error bars (where visible) are the standard deviation. Photo-cross-linking activity of the wild-type FabF is set to 100%.

selected as new positions for pBpa installation. The Asp35pBpa and Leu37pBpa mutants of AcpP were prepared as described previously for AcpP-Ser36pBpa. CD spectra for apo-AcpP-Asp35pBpa and apo-AcpP-Leu37pBpa matched closely to that of the wild-type AcpP (Figure S3C), suggesting similar secondary structures. Next, as mimics of an extender unit modified carrier protein and an extended fatty acid intermediate,[20] the corresponding malonyl- and octanoyl-form of each Asp35pBpa and Leu37pBpa AcpP mutant was prepared via the broad specificity phosphopantetheinyl transferase, Sfp. After initially screening photo-cross-linking efficiencies of each AcpP variant with the wild-type FabF, AcpP-Leu37pBpa was selected based on its higher photo-cross-linking efficiency compared to AcpP-Asp35pBpa (data not shown).

Next, malonyl- and octanoyl-AcpP-Leu37pBpa were subjected to photo-cross-linking with each member of the previously described panel of FabF surface mutants. The cross-linking efficiencies of malonyl-AcpP-Leu37pBpa and octanoyl-AcpP-Leu37pBpa were very similar to each other with most of the FabF surface mutants tested (Figure 5). Notably, the photo-cross-linking efficiency for the FabF-Cys163Ala mutant with malonyl-AcpP-Leu37pBpa as the potential interaction partner was ∼3-fold higher than that with octanoyl-AcpP-Leu37pBpa as the interaction partner. Curiously, identified as the site on FabF responsible for tethering the growing fatty acid chain from AcpP during chain transfer,[19] Cys163 is essential for the chain transfer process but has been shown not to be involved in the decarboxylation of malonyl-ACP.[21] Thus, the observation that AcpP-malonylation supports higher photo-cross-linking with FabF-Cys163Ala than AcpP-octanoylation might reflect the different contribution of Cys163 in the binding interface with AcpP during the catalytic cycle of FabF. Another notable observation is that FabF-Arg206Lys supports photo-cross-linking efficiency of ∼60% with both malonyl- and octanoyl-AcpP-Leu37pBpa. This contrasts sharply to the complete lack of detectable photo-cross-linking when pBpa is installed at the phosphopantetheinylation site of AcpP (Figure 4), implying that AcpP-acylation is capable of rescuing the faulty FabF-Arg206Lys:AcpP interaction. Taken together, these results suggest that the FabF binding interface involved in transacylation and condensation with AcpP are similar.

Probing Contribution of a Conserved Carrier Protein Motif to the FabF Binding Interface. The carrier protein phosphopantetheinylation site is part of a highly conserved Asp-Ser-Leu (DSL) motif at the N-terminus of helix II, located on the carrier protein surface (Figure 3). This motif has been implied to be involved in protein interactions between the ACP and its various interaction partners (Table S4), although little is known regarding interactions with FabF.[22,23] The pBpa-based photo-cross-linking assay was used to probe contribution of the DSL motif to the FabF binding interface. To circumvent production of each subsequent carrier protein alanine mutant as a pBpa-modified mutant protein, we hypothesized that pBpa

dx.doi.org/10.1021/bi500936u | *Biochemistry* 2014, 53, 7494−7502

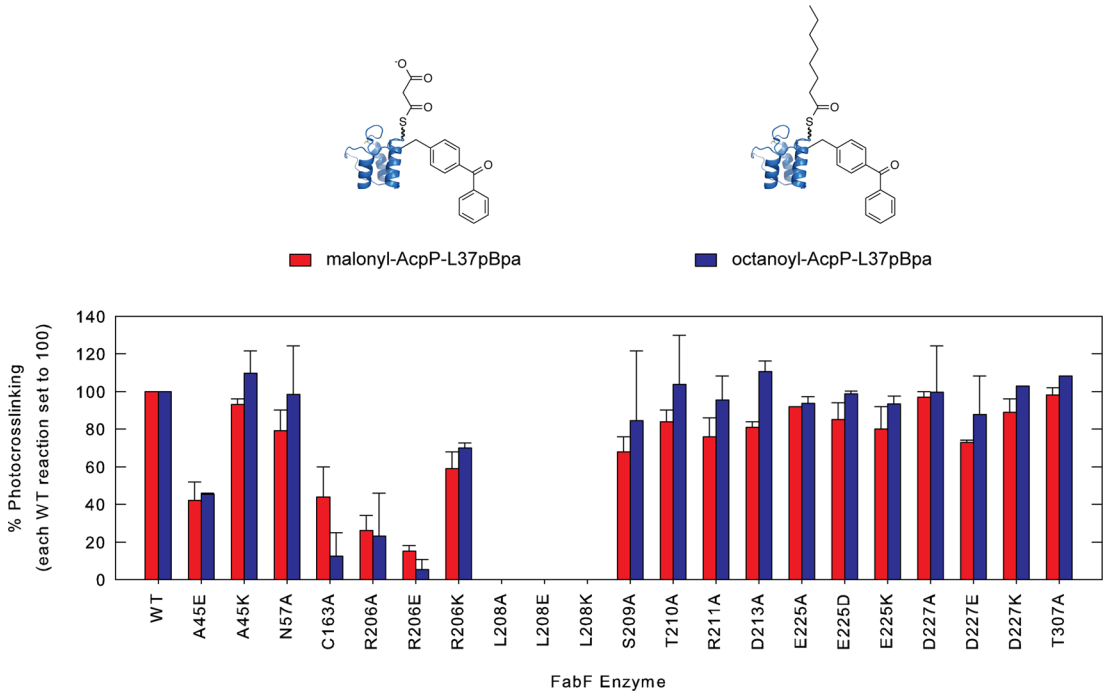

Figure 5. Photo-cross-linking activities of acylated-AcpP and a panel of FabF surface mutants. Data are the average percentage (%) photo-cross-linking of wild-type or mutant FabF using malonyl- or octanoyl-AcpP-Leu37pBpa, error bars (where visible) are the standard deviation (n = 2). Photo-cross-linking activity of the wild-type FabF is set to 100% for each acyl-form of AcpP.

could instead be introduced into FabF, and a single pBpa-modified FabF would then be used to probe interactions with a set of carrier protein mutants (Figure 1b). FabF residues Arg206 and Leu208 are likely key residues involved in the interaction with AcpP (Figure 4), and these two sites were initially elected for pBpa installation. Expression of FabF-Arg206Ala was significantly higher than that of FabF-Leu208Ala (data not shown). Subsequently, FabF-Arg206pBpa was overexpressed, purified to homogeneity, and the identity confirmed by ESI-MS analysis (Table S3 and Figure S4). The secondary structure of FabF-Arg206pBpa was not significantly different from that of the wild-type FabF, as judged by CD spectroscopy (Figure S3D). Gratifyingly, upon photo-cross-linking FabF-Arg206pBpa in the presence of apo-AcpP, a higher molecular weight protein band consistent with the expected mass of the photo-cross-linked FabF-AcpP was observed (Table 2 and Figure S5). The percentage photo-cross-linking for FabF-Arg206pBpa and apo-AcpP (33%, Table 2) was less than half of that for AcpP-Ser36pBpa in the presence of FabF (Table 1). The difference in photo-cross-linking efficiency might be attributed to the inherent flexibility of AcpP,[18] which could allow it to present pBpa at a position better suited for photo-cross-linking with FabF, while the FabF structure is likely more rigid than AcpP.[16,19] Upon incubation of FabF-Arg206pBpa with other members of the ACP panel, cross-linking was only detected with apo-Sc-FAS-ACP (29%) (Table 2 and Figure S5), consistent with the photo-cross-linking profile when AcpP is modified with pBpa (Table 1). In conclusion, these data demonstrate that pBpa-modified FabF can be used to report orthogonal carrier proteins interactions in the same way as the analogous strategy using pBpa-modified carrier protein. This demonstration now enables the contribution of the conserved DSL motif to recognition by FabF to be interrogated.

Table 2. Cross-Linking Efficiency between FabF-Arg206pBpa and a Panel of ACP's[a]

ACP	$ACP2_{DEBS}$	$ACP6_{DEBS}$	Act-ACP	AcpP	Sc-FAS-ACP
% photo-cross-linking	N.D.	N.D.	N.D.	33	29

[a]Each ACP was used in the apo form. N.D., not detected.

Accordingly, the Asp35Ala and Leu37Ala mutants of AcpP were constructed, overexpressed, and purified as their *apo*-forms. The secondary structures of Asp35Ala and Leu37Ala were not significantly different from the wild-type *apo*-AcpP, as judged by CD spectroscopy (Figure S3E). Next, the AcpP mutants Asp35Ala and Leu37Ala were each incubated with FabF-Arg206pBpa and examined for photo-cross-linking. Notably, Asp35Ala displayed ∼5-fold lower photo-cross-linking efficiency, compared to the wild-type apo-AcpP, while the poor photo-cross-linking activity of the Leu37Ala mutant was difficult to distinguish from the background of the assay (Figure 6). These results suggest that both Asp35 and Leu37 play an intimate role in recognition by FabF.

Probing the Contribution of the Carrier Protein Acyl Moiety to the FabF Binding Interface. It has been suggested that intermediates covalently attached to AcpP mediate specific conformational changes in the carrier protein that may orchestrate protein−protein interactions during the FAS catalytic cycle.[4,24] Structural studies of acylated forms of AcpP have revealed important observations, including (1) a hydrophobic core sequesters elongating acyl chains[24,25] and requires conformational changes to release the acyl intermediate for delivery,[1,4] and (2) the AcpP structure is not significantly perturbed upon phosphopantetheinylation.[26] Yet, very little is known regarding modulation of the FabF binding interface via AcpP acylation.

dx.doi.org/10.1021/bi500936u | *Biochemistry* 2014, 53, 7494−7502

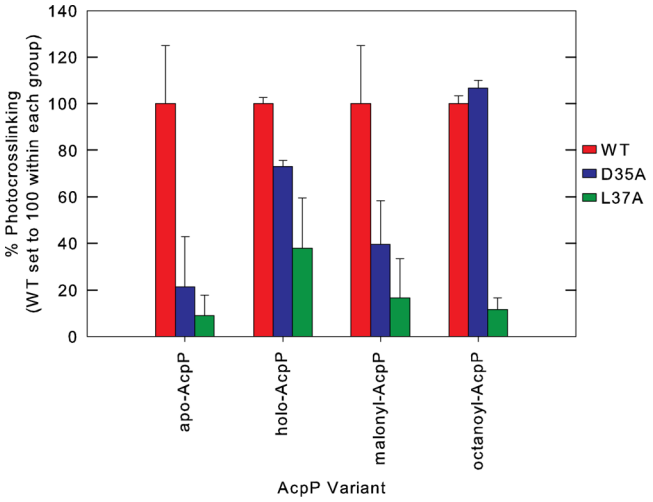

Figure 6. Photo-cross-linking activities of various acylated forms of AcpP. Each variant of the wild-type and mutant AcpP were prepared as described in the Materials and Methods and photo-cross-linked in the presence of FabF-Arg206pBpa. Data are the average percent (%) photo-cross-linking activities of two independent measurements, error bars represent ± standard deviation from the mean (n = 2). Photo-cross-linking activity of the wild-type AcpP is set to 100% within each apo, holo, malonyl, and octanoyl group.

In order to probe the potential influence of AcpP-acylation on protein interactions with FabF, the holo-, malonyl-, and octanoyl-derivatives of the wild-type AcpP, Asp35Ala, and Leu37Ala mutants were prepared via Sfp-mediated phosphopantetheinylation from the corresponding acyl-CoA. However, even with excess Sfp, it proved difficult to afford the acylated AcpPs in quantitative yield when the Asp35Ala and Leu37Ala mutants were used (data not shown). Nevertheless, each acyl-AcpP was subjected to photo-cross-linking with FabF-Arg206pBpa, and the photo-cross-linking efficiencies of the wild-type, Asp35Ala, and Leu37Ala AcpP were compared to each other within each holo-, malonyl-, and octanoyl-group.

The photo-cross-linking efficiency of holo-AcpP-Asp35Ala was ∼70% that of holo-AcpP, while holo-AcpP-Leu37Ala displayed one-third the photo-cross-linking efficiency of holo-AcpP (Figure 6). Interestingly, Leu37 is proposed to take part in hydrophobic interactions with the hydrophobic region of the phosphopantetheine moiety.[27] In addition, Leu37 in ACP's from several systems is likely directly involved in hydrophobic interactions with other interaction partners (Table S4). Perhaps substitution of Leu37 negatively impacts the binding interface with FabF through disruption of similar hydrophobic interactions. The photo-cross-linking efficiencies of the malonyl-AcpP panel are similar to those of the holo-AcpP set (Figure 6), consistent with an NMR study that showed the holo- and malonyl-ACP from a type II PKS share similar structural features.[28] Notably, variants of the octanoyl-AcpP series displayed different photo-cross-linking behavior compared to those within the holo- and malonyl-variants. In contrast to the holo- and malonyl-AcpP's, wild-type octanoyl-AcpP and octanoyl-AcpP-Asp35Ala displayed similar photo-cross-linking efficiencies to each other. However, the photo-cross-linking efficiency for octanoyl-AcpP-Leu37Ala remained poor in comparison to the wild-type and Asp35Ala octanoyl-AcpP (Figure 6). These data suggest that structural changes that accompany AcpP-octanoylation potentially play a role in rescuing the faulty binding interface between FabF and the AcpP mutant, Asp35Ala. The absence of improvement in photo-cross-linking efficiency of AcpP-Leu37Ala upon octanoylation could be attributed to the disturbance of the proposed hydrophobic interaction between Leu37 and the phosphopantetheine moiety.[27] Taken together, these data suggest that AcpP-acylation can impact the interaction between Leu37 and phosphopantetheine, and that Asp35 plays an important role in the binding interface with FabF.

DISCUSSION

ACP's are involved in critical protein interactions with a variety of FAS and PKS catalytic domains. Probing the molecular basis of such delicately orchestrated protein interactions is key to understanding the mechanism and specificity that are the hallmark of the programmed biosynthetic assembly of fatty acids and polyketides. The difficulty of probing and interrogating the weak and transient interactions between ACP's and KS's is exemplified by the ongoing elegant work of Burkart and co-workers, which relies on the design and synthesis of specific mechanism-based probes that covalently cross-link the ACP and cognate interaction partner.[4,5,29,30] Clearly, additional tools need to be developed and evaluated for studying protein interactions among FAS's and PKS's, particularly for those biosynthetic systems with unusual substrate specificities, whereby effective cross-linkers might be difficult to discover. Macromolecular interactions of proteins in other biological systems have often been probed via the introduction of photo-cross-linking unnatural amino acids.[31−33] However, until very recently,[10] the incorporation of unnatural amino acids into FAS's or PKS's had not been reported. Here, we significantly expanded our previously reported strategy for probing ACP interactions by expressing the *E. coli* FAS proteins AcpP and FabF with site-specifically introduced pBpa in combination with Sfp-catalyzed modification of the ACP. To the best of our knowledge, there are currently no crystal structures that describe the AcpP:FabF binding interaction or that of any other ACP:KS complex.

Subsequently, our pBpa-based photo-cross-linking assay was first expanded to faithfully report a broad panel of ACP:FabF interactions, including ACP's from a type I PKS, type II PKS, and type II FAS pathways. The data from this expanded ACP panel highlighted the electrostatic contribution of H_{II} to the AcpP:FabF interaction. In addition, a carrier protein from the FAS of *S. coelicolor* was identified to be a potential substrate for the *E. coli* FabF based on photo-cross-linking. Consistent with the postulated role of H_{II}, the Sc-FAS-ACP shares three conserved glutamates in H_{II} with AcpP. Additionally, $ACP6_{DEBS}$ was identified as a poor interaction partner for FabF, which is likely attributed to its neutral H_{II} surface. Conspicuously, carrier proteins among our tested panel with positively charge residues at equivalent positions to glutamates in H_{II} of AcpP failed to provide detectable photo-cross-linking.

To the best of our knowledge, the AcpP:FabF binding interface has not been previously experimentally mapped. Accordingly, surface scanning mutagenesis and photo-cross-linking was used to identify FabF residues that contribute to the AcpP:FabF binding interface, using an expanded set of surface positions and mutations than reported in our previous proof-of-principle study.[10] Gratifyingly, photo-cross-linking efficiency between pBpa-modified AcpP and mutant FabF is incredibly sensitive to the location of amino acid substitution. This is likely a result of the small reaction sphere of the reactive intermediate, estimated at ∼3.1 Å.[17] Subsequently, Arg206 and

dx.doi.org/10.1021/bi500936u | *Biochemistry* 2014, 53, 7494−7502

Leu208 were found to be key residues that contribute to the AcpP:FabF binding interaction, while residues located distant from these two sites, or even immediately adjacent (e.g., Ser209, Figure 4), were far less sensitive to amino acid substitution, as judged by photo-cross-linking.

One particular advantage of our approach is that once a pBpa installation site on AcpP (or FabF) is identified that leads to efficient photo-cross-linking, the phosphopantetheinylation site is available for modification with virtually any molecule, via Sfp. In this way, the FabF epitopes involved in transacylation vs condensation were probed by preparing malonyl- and octanoyl-AcpP, respectively. The transacylation and condensation epitopes were found to be similar, at least among the FabF surface residues tested. The known requirement of Cys163 for transacylation but not for chain elongation[21] was also reflected in the photo-cross-linking assay using Cys163Ala and the acylated AcpP's.

The ability to relocate the pBpa installation site was further leveraged to probe the importance of the conserved AcpP DSL motif. Previous studies citing ACP's from diverse systems support involvement of the DSL motif in various protein interactions,[1,23] but little is known regarding involvement with KS's such as FabF. Mutagenesis of the DSL motif, in combination with photo-cross-linking using pBpa-modified FabF, led to confirmation that Asp and Leu in the DSL motif play integral roles in maintaining the FabF:AcpP binding interface. Perhaps more unexpectedly, the AcpP-Asp35Ala:-FabF interaction could be rescued by octanoylation of the AcpP, whereas that for AcpP-Leu37Ala could not. These data are consistent with the notion that Leu37 interacts with the phosphopantetheine dimethyl group[27] and that disruption of this interaction via amino acid substitution cannot be rescued by octanoylation.

In summary, this study expanded the utility of our previously reported photo-cross-linking strategy for probing and interrogating the molecular basis for protein interactions between AcpP and FabF. The FabF epitope involved in forming the AcpP:FabF binding interface was mapped with single residue resolution, and the influence of AcpP-acylation determined. Photo-cross-linking also established the intimate contribution of the conserved DSL in maintenance of the AcpP:FabF interaction. These data highlight photo-cross-linking as a powerful tool for probing and interrogating protein interactions in complex biosynthetic apparatus. In the future, we expect this strategy will be applied to other protein interactions that involve ACP's, particularly those that require complex or difficult to synthesize substrates that would otherwise be difficult to probe using cross-linking reagents and crystallography. Additionally, we expect that more detail regarding such binding interfaces could be revealed by coupling our photo-cross-linking approach with multiplexed mass spectrometry.[34]

■ ASSOCIATED CONTENT

Supporting Information

Supplemental tables and figures. This material is available free of charge via the Internet at http://pubs.acs.org.

■ AUTHOR INFORMATION

Corresponding Author

*E-mail: gjwillia@ncsu.edu.

Present Address

†(Z.Y.) Department of Biomedical Engineering, Duke University, Durham, NC, 27708.

Funding

This study was supported by a National Science Foundation CAREER award (CHE-1151299 to G.J.W.).

Notes

The authors declare no competing financial interest.

■ ACKNOWLEDGMENTS

We thank the Biological Core Instrumentation Facility in the Department of Chemistry at North Carolina State University.

■ ABBREVIATIONS

ACP, acyl carrier protein; FAS, fatty acid synthase; KS, ketosynthase; pBpa, *p*-benzoyl-L-phenylalanine; PKS, polyketide synthase

■ REFERENCES

(1) Crosby, J., and Crump, M. P. (2012) The structural role of the carrier protein — active controller or passive carrier. *Nat. Prod. Rep. 29*, 1111−1137.

(2) Abe, I., and Morita, H. (2010) Structure and function of the chalcone synthase superfamily of plant type III polyketide synthases. *Nat. Prod. Rep. 27*, 809−838.

(3) Song, L., Barona-Gomez, F., Corre, C., Xiang, L., Udwary, D. W., Austin, M. B., Noel, J. P., Moore, B. S., and Challis, G. L. (2006) Type III polyketide synthase beta-ketoacyl-ACP starter unit and ethylmalonyl-CoA extender unit selectivity discovered by Streptomyces coelicolor genome mining. *J. Am. Chem. Soc. 128*, 14754−14755.

(4) Nguyen, C., Haushalter, R. W., Lee, D. J., Markwick, P. R., Bruegger, J., Caldara-Festin, G., Finzel, K., Jackson, D. R., Ishikawa, F., O'Dowd, B., McCammon, J. A., Opella, S. J., Tsai, S. C., and Burkart, M. D. (2014) Trapping the dynamic acyl carrier protein in fatty acid biosynthesis. *Nature 505*, 427−431.

(5) Bruegger, J., Haushalter, B., Vagstad, A., Shakya, G., Mih, N., Townsend, C. A., Burkart, M. D., and Tsai, S. C. (2013) Probing the selectivity and protein•protein interactions of a nonreducing fungal polyketide synthase using mechanism-based crosslinkers. *Chem. Biol. 20*, 1135−1146.

(6) Zhang, Y. M., Rao, M. S., Heath, R. J., Price, A. C., Olson, A. J., Rock, C. O., and White, S. W. (2001) Identification and analysis of the acyl carrier protein (ACP) docking site on beta-ketoacyl-ACP synthase III. *J. Biol. Chem. 276*, 8231−8238.

(7) Beltran-Alvarez, P., Arthur, C. J., Cox, R. J., Crosby, J., Crump, M. P., and Simpson, T. J. (2009) Preliminary kinetic analysis of acyl carrier protein-ketoacylsynthase interactions in the actinorhodin minimal polyketide synthase. *Mol. Biosyst. 5*, 511−518.

(8) Angelini, S., My, L., and Bouveret, E. (2012) Disrupting the Acyl Carrier Protein/SpoT interaction in vivo: identification of ACP residues involved in the interaction and consequence on growth. *PLoS One 7*, e36111.

(9) Weissman, K. J., Hong, H., Popovic, B., and Meersman, F. (2006) Evidence for a protein-protein interaction motif on an acyl carrier protein domain from a modular polyketide synthase. *Chem. Biol. 13*, 625−636.

(10) Ye, Z., Bair, M., Desai, H., and Williams, G. J. (2011) A photocrosslinking assay for reporting protein interactions in polyketide and fatty acid synthases. *Mol. BioSyst. 7*, 3152−3156.

(11) Yin, J., Lin, A. J., Golan, D. E., and Walsh, C. T. (2006) Site-specific protein labeling by Sfp phosphopantetheinyl transferase. *Nat. Protoc 1*, 280−285.

(12) Greenfield, N. J. (2006) Using circular dichroism spectra to estimate protein secondary structure. *Nat. Protoc 1*, 2876−2890.

(13) Revill, W. P., Bibb, M. J., and Hopwood, D. A. (1996) Relationships between fatty acid and polyketide synthases from

Streptomyces coelicolor A3(2): characterization of the fatty acid synthase acyl carrier protein. *J. Bacteriol. 178*, 5660−5667.
(14) Crump, M. P., Crosby, J., Dempsey, C. E., Parkinson, J. A., Murray, M., Hopwood, D. A., and Simpson, T. J. (1997) Solution structure of the actinorhodin polyketide synthase acyl carrier protein from Streptomyces coelicolor A3(2). *Biochemistry 36*, 6000−6008.
(15) Tang, Y., Lee, T. S., Kobayashi, S., and Khosla, C. (2003) Ketosynthases in the initiation and elongation modules of aromatic polyketide synthases have orthogonal acyl carrier protein specificity. *Biochemistry 42*, 6588−6595.
(16) Qiu, X., and Janson, C. A. (2004) Structure of apo acyl carrier protein and a proposal to engineer protein crystallization through metal ions. *Acta Crystallogr. D Biol. Crystallogr. 60*, 1545−1554.
(17) Dorman, G., and Prestwich, G. D. (1994) Benzophenone photophores in biochemistry. *Biochemistry 33*, 5661−5673.
(18) Chan, D. I., Stockner, T., Tieleman, D. P., and Vogel, H. J. (2008) Molecular dynamics simulations of the Apo-, Holo-, and acyl-forms of Escherichia coli acyl carrier protein. *J. Biol. Chem. 283*, 33620−33629.
(19) Huang, W., Jia, J., Edwards, P., Dehesh, K., Schneider, G., and Lindqvist, Y. (1998) Crystal structure of beta-ketoacyl-acyl carrier protein synthase II from E.coli reveals the molecular architecture of condensing enzymes. *EMBO J. 17*, 1183−1191.
(20) Edwards, P., Nelsen, J. S., Metz, J. G., and Dehesh, K. (1997) Cloning of the fabF gene in an expression vector and in vitro characterization of recombinant fabF and fabB encoded enzymes from *Escherichia coli*. *FEBS Lett. 402*, 62−66.
(21) McGuire, K. A., Siggaard-Andersen, M., Bangera, M. G., Olsen, J. G., and von Wettstein-Knowles, P. (2001) Beta-Ketoacyl-[acyl carrier protein] synthase I of *Escherichia coli*: aspects of the condensation mechanism revealed by analyses of mutations in the active site pocket. *Biochemistry 40*, 9836−9845.
(22) Zhang, Y. M., Wu, B., Zheng, J., and Rock, C. O. (2003) Key residues responsible for acyl carrier protein and beta-ketoacyl-acyl carrier protein reductase (FabG) interaction. *J. Biol. Chem. 278*, 52935−52943.
(23) Xu, W., Qiao, K., and Tang, Y. (2013) Structural analysis of protein-protein interactions in type I polyketide synthases. *Crit. Rev. Biochem. Mol. Biol. 48*, 98−122.
(24) Ploskon, E., Arthur, C. J., Kanari, A. L., Wattana-amorn, P., Williams, C., Crosby, J., Simpson, T. J., Willis, C. L., and Crump, M. P. (2010) Recognition of intermediate functionality by acyl carrier protein over a complete cycle of fatty acid biosynthesis. *Chem. Biol. 17*, 776−785.
(25) Roujeinikova, A., Simon, W. J., Gilroy, J., Rice, D. W., Rafferty, J. B., and Slabas, A. R. (2007) Structural studies of fatty acyl-(acyl carrier protein) thioesters reveal a hydrophobic binding cavity that can expand to fit longer substrates. *J. Mol. Biol. 365*, 135−145.
(26) Kim, Y., Kovrigin, E. L., and Eletr, Z. (2006) NMR studies of Escherichia coli acyl carrier protein: dynamic and structural differences of the apo- and holo-forms. *Biochem. Biophys. Res. Commun. 341*, 776−783.
(27) Evans, S. E., Williams, C., Arthur, C. J., Burston, S. G., Simpson, T. J., Crosby, J., and Crump, M. P. (2008) An ACP structural switch: conformational differences between the apo and holo forms of the actinorhodin polyketide synthase acyl carrier protein. *ChemBioChem 9*, 2424−2432.
(28) Evans, S. E., Williams, C., Arthur, C. J., Ploskon, E., Wattana-amorn, P., Cox, R. J., Crosby, J., Willis, C. L., Simpson, T. J., and Crump, M. P. (2009) Probing the Interactions of early polyketide intermediates with the Actinorhodin ACP from S. coelicolor A3(2). *J. Mol. Biol. 389*, 511−528.
(29) Worthington, A. S., Porter, D. F., and Burkart, M. D. (2010) Mechanism-based crosslinking as a gauge for functional interaction of modular synthases. *Org. Biomol. Chem. 8*, 1769−1772.
(30) Worthington, A. S., Rivera, H., Torpey, J. W., Alexander, M. D., and Burkart, M. D. (2006) Mechanism-based protein cross-linking probes to investigate carrier protein-mediated biosynthesis. *ACS Chem. Biol. 1*, 687−691.
(31) Ray-Saha, S., Huber, T., and Sakmar, T. P. (2014) Antibody epitopes on g protein-coupled receptors mapped with genetically encoded photoactivatable cross-linkers. *Biochemistry 53*, 1302−1310.
(32) Majmudar, C. Y., Lee, L. W., Lancia, J. K., Nwokoye, A., Wang, Q., Wands, A. M., Wang, L., and Mapp, A. K. (2009) Impact of nonnatural amino acid mutagenesis on the in vivo function and binding modes of a transcriptional activator. *J. Am. Chem. Soc. 131*, 14240−14242.
(33) Mori, H., and Ito, K. (2006) Different modes of SecY-SecA interactions revealed by site-directed in vivo photo-cross-linking. *Proc. Natl. Acad. Sci. U.S.A. 103*, 16159−16164.
(34) Majmudar, C. Y., Wang, B., Lum, J. K., Hakansson, K., and Mapp, A. K. (2009) A high-resolution interaction map of three transcriptional activation domains with a key coactivator from photo-cross-linking and multiplexed mass spectrometry. *Angew. Chem., Int. Ed. Engl. 48*, 7021−7024.